Published in final edited form as:
Neuron. 2006 July 6; 51(1): 125–134. doi:10.1016/j.neuron.2006.05.025.

Dorsal Premotor Neurons Encode the Relative Position of the Hand, Eye, and Goal during Reach Planning

Bijan Pesaran[1,*], **Matthew J. Nelson**[1], and **Richard A. Andersen**[1]
[1]Division of Biology, California Institute of Technology, Pasadena, California 91125

Summary

When reaching to grasp an object, we often move our arm and orient our gaze together. How are these movements coordinated? To investigate this question, we studied neuronal activity in the dorsal premotor area (PMd) and the medial intraparietal area (area MIP) of two monkeys while systematically varying the starting position of the hand and eye during reaching. PMd neurons encoded the relative position of the target, hand, and eye. MIP neurons encoded target location with respect to the eye only. These results indicate that whereas MIP encodes target locations in an eye-centered reference frame, PMd uses a relative position code that specifies the differences in locations between all three variables. Such a relative position code may play an important role in coordinating hand and eye movements by computing their relative position.

Introduction

Reaching to a pick up a cup often involves not only generating a pattern of muscle activity in the arm that will move the limb and grasp the cup, but also coordinating a movement of the eyes to the same place. These visually-guided movements require sensory-motor transformations to convert incoming visual information about target location into outgoing patterns of muscle activity (Andersen and Buneo, 2002; Kalaska et al., 1997; Shadmehr and Wise, 2005). Work investigating reference frames has been useful for understanding the transformations needed to guide individual movements of the hand and eye. In contrast, the reference frames involved in coordinating these movements are likely to play a major role in understanding interactions between the saccadic and reach systems but have received relatively little attention.

One reason for this dearth of investigation is that reference frames are usually defined as centered on individual body parts, such as the eye or hand, rather than multiple body parts. Eye-centered reference frames have been found in single-cell activity in eye movement areas (Barash et al., 1991b; Goldberg and Bruce, 1990; Mays and Sparks, 1980) and in the parietal reach region (PRR) of posterior parietal cortex (PPC) which is at an early stage of the reaching pathway (Batista et al., 1999). Eye-centered dependence during movement plans has also been reported in human imaging studies (DeSouza et al., 2000; Medendorp et al., 2003; Merriam et al., 2003; Sereno et al., 2001) and human lesion studies (Duhamel et al., 1992; Khan et al., 2005). Reference frames centered on other body parts, such as the hand, are stable across eye movements and are well suited for the motor output stage of reaches (Graziano and Gross, 1998). Such body-part-centered reference frames are thought to be present in the dorsal premotor (Caminiti et al., 1990, 1991; Crammond and Kalaska, 1994; Fu et al., 1993; Johnson et al., 1996; Shen and Alexander, 1997) (PMd) and ventral

*Correspondence: bijan@vis.caltech.edu.

premotor (Fogassi et al., 1992; Graziano et al., 1994; Kakei et al., 2001) (PMv) areas of frontal cortex.

Here, we investigate reference frames that can be centered on multiple body parts as well as just one body part. For example, we can define a reference frame centered on the hand, the eye, and the relative position of the hand with respect to the eye. In such an encoding, the same activity is present when the three variables, hand, eye, and target, have a particular configuration, even though they may occupy different absolute positions in space. Relative position is also useful for performing the sensory-motor transformations between spatial systems defined in extrinsic space which may be useful for coordination. This is because, in extrinsic space, a relative position reference frame can be used to go directly from an eye-centered reference frame into a hand-centered reference frame and back again (Buneo and Andersen, 2005).

To see whether eye position signals in premotor cortex are combined with hand and target position in a relative position code, we recorded a population of neurons in the PMd cortex of two monkeys during a delayed reach task in which we independently varied the position of the eye, hand, and target across a range of locations. Another population of neurons in MIP was recorded under identical conditions for comparison. Although we identify these signals during a reach without a saccade, we propose that they could allow coordination of reaches with saccades.

Results

Behavioral Task and Reference Frame Analysis

Movement commands can be represented in two complementary spaces—an extrinsic space given by the endpoints of movements and an intrinsic space given by the joint angles and muscle activations needed to achieve the movement endpoint. While eye and arm movements have distinct intrinsic spaces, they can be considered to share a common extrinsic space where both movements can be coordinated. Figure 1A shows the geometry of the extrinsic space in which our data was analyzed. The intrinsic motor commands for the saccade can be transformed from the position of the target with respect to the eye in extrinsic coordinates, T_E, while the intrinsic motor commands for the reach can be transformed from the position of the target with respect to the hand in extrinsic coordinates, T_H. These extrinsic movement vectors are related to each other through another extrinsic vector, the relative position of the hand and eye, which can equally be viewed as hand position with respect to the eye or eye position with respect to the hand (H_E and E_H). We will refer to this vector as H_E, equivalent to the hand in eye coordinates (Buneo and Andersen, 2005). To coordinate hand and eye movements, the brain needs to integrate these pieces of information so neural responses can depend on eye position, hand position, and target position. For a more detailed analysis of the relationship between these variables and intrinsic coordinates, see (Soechting et al., 1995; Tweed and Vilis, 1987).

Since all three vectors may be simultaneously represented in single-cell activity, we developed a reference frame dissociation task (Figure 1B) to independently control eye, hand, and target position and then analyzed neuronal responses to all three variables. In this task, we instructed eye and hand position to one of four locations and then instructed a delayed reach without a saccade to a target at one of four positions above or below the starting point (see Experimental Procedures). Independently controlling each variable across a range of values was necessary to allow us to determine the spatial reference frame by distinguishing between a representation of the target in eye coordinates, the target in hand coordinates, and the relative position of the hand and eye.

The panels of Figure 2 illustrate three idealized neuronal responses to the reference frame dissociation task, each illustrating a different reference frame. The firing rate is modeled as a Gaussian response field and, in Figures 2A and 2B, multiplied by a monotonic "gain field" (Andersen et al., 1985; see Experimental Procedures). Responses are represented as three two-dimensional matrices at the response field peak consisting of the firing rate at each of four target and eye positions (target-eye, TE), eye and hand positions (hand-eye, HE) and target and hand positions (target-hand, TH). The eye-centered cell has a reference frame centered on the eye with a gain field of hand position and encodes the vector T_E (Figure 2A). The hand-centered cell has a reference frame centered on the hand with a gain field of eye position and encodes the vector T_H (Figure 2B). The relative position cell has a reference frame centered on the hand and eye so that the activity encodes the relative position of the hand and eye and encodes three vectors, T_E, T_H, and H_E (Figure 2C).

Intuitively, when we talk about the reference frame of a cell, we are referring to a set of task conditions for which the response of the cell stays approximately the same. In the case of the eye-centered cell, the response is the same whenever the target and the eye are in the same position with respect to each other. When the target is moved to a new location, the eye also needs to be moved to maintain the response. For this case, changes in response to the position of the target and the eye cannot be separated from each other. In contrast, for an eye-centered cell, the position of the hand can also have an influence, but this influence is multiplicative, scaling the response up or down. Since multiplicative modulations cannot be compensated for by shifting another variable, we can separate hand position from the other variables. Consequently, according to this logic, we first need to identify which pairs of variables are separable from each other, and then we focus on how much the inseparable variables need to be moved with respect to each other to maintain the response.

Given this, we test the reference frame of each cell using a two step procedure that is applied to each of the three response matrices (see Experimental Procedures). The first step involves determining whether the variables in question are separable using a singular value decomposition (SVD) of the response matrix. The second step is to measure the response field orientation, determined from a gradient analysis. Separability decides whether the variables combine in a gain field. If the response is inseparable, then the response field orientation is useful for quantifying how much the response shifts as the variables are changed. The combination of these techniques allows us to differentiate between potential reference frames.

For the idealized responses, the eye-centered cell has an inseparable TE response whose orientation is −90°, a separable HE response whose orientation is 177°, and a separable TH response whose orientation is 3° (Figure 2A). The hand-centered cell has a separable TE response whose orientation is −3°, a separable HE response whose orientation is −3°, and an inseparable TH response whose orientation is −90° (Figure 2B). The relative position cell has inseparable TE, HE, and TH responses all of whose orientations are −90° (Figure 2C). Note that while gain fields can modulate the responses (see, for example, the HE plot of the eye-centered cell), they cannot make them inseparable. In contrast, inseparable encoding of a pair of variables with a response field orientation of −90° indicates the encoding is a vector and not a gain field.

Separable and Inseparable Eye-Hand-Target Tuning

We recorded the activity of 111 PMd neurons (73 Monkey Z, 38 Monkey E) and 48 MIP neurons (42 Monkey Z, 6 Monkey E) during the reference frame dissociation task to determine the reference frame of cells in each area (Figure 1B; Experimental Procedures). Figure 3 shows the response of an example PMd cell during this task. Changing hand or eye position for a given target position results in a robust change in firing, visible by comparing

rasters of the same color across neighboring panels either within rows or columns. Similar changes in firing are also present when changing target position for a given hand and eye position, visible by comparing rasters of different colors in the same panel.

Figure 4 shows the TE, HE, and TH response matrices for the example PMd cell in Figure 3 at the peak of the response field during the delay period. Plotting the data in this way shows how the TE response is suppressed for the target to the right of the eye and increases as the target is moved further to the left of the eye. Similar effects are present for the HE and TH responses. By analyzing the TE, HE, and TH response matrices, we found the TE, HE, and TH responses were inseparable for this cell ($p < 0.05$) and the orientations were all diagonal, with a dominance of eye and hand position over target position (TE response field orientation, −130°, Figure 4D; HE response field orientation, −77°, Figure 4E; TH response field orientation, −146°, Figure 4F). Since all the variable pair responses are inseparable for this cell, the influence of one variable on another is not due to a gain field modulating a response centered on one variable. Therefore, this cell is a relative position cell.

Figure 5 shows the response of an example MIP neuron to the reference frame dissociation task. Unlike the PMd cell, large changes in firing are only present when changing eye position for a given target position, visible by comparing rasters of the same color across panels in different rows or target position for a given eye position, visible by comparing rasters of different colors within a row. Changing hand position alone does not result in a large change in firing rate.

The TE, TH, and HE response matrices for the example MIP neuron let us analyze this pattern (Figure 6). Similar to the PMd cell response, the TE response for the example MIP neuron was inseparable (Figure 6A) with a response field orientation of −86° (Figure 6D). In contrast, the TH and HE responses for this cell were separable (Figures 6B and 6C). The TH response was dominated by target position (TH response field orientation, 0°, Figure 6E) with little effect of hand position. The HE response was dominated by eye position (HE response field orientation, 177°, Figure 6F) again with little effect of hand position. Therefore, this cell is an eye-centered cell and represents target position with respect to eye position alone, in agreement with previously published reports (Batista et al., 1999;Buneo et al., 2002).

Analysis of the delay period responses across a population of neurons in each area reinforced the distinction that PMd neurons had a relative position code while MIP neurons had an eye-centered code (Figure 7). Across the population, a majority of PMd neurons were tuned to the TE variable pair (63/111 [57%], $p < 0.05$, randomization test [see Experimental Procedures]), as well as the TH variable pair (63/111 [57%]) and the HE variable pair (58/111 [52%]) tuning. The number of cells tuned to each variable pair is different because some cells were tuned to only one of the three variables. Tuned TE, TH, and HE responses of PMd neurons were mostly inseparable (Figure 7A; TE, 42/63 [67%]; TH, 38/63 [60%]; HE, 40/58 [69%]; $p < 0.05$), indicating that a gain field mechanism could not account for the responses of these neurons. Analysis of the response field orientation for these inseparable cells showed that the mean response field orientations pointed down (Figures 7B–7D; TE, −81°; TH, −79°; HE, −98°). This means that response fields almost completely shifted when either of the hand, eye, or target was moved with respect one of the other variables.

Across the population of 48 MIP neurons, 33 cells showed TE tuning (69%), 41 cells showed TH tuning (85%), and 28 cells showed HE tuning (58%). The distribution of separable and inseparable responses for these tuned MIP neurons was markedly different than that of PMd neurons (Figure 7E). Only the TE responses were mainly inseparable (24/33 [73%] inseparable), while the HE and TH responses were mainly separable (HE,

20/28 [71%] separable; TH, 22/41 [54%] separable). Similar to the example MIP cell, the average TE response field orientation for tuned MIP neurons was −94°, indicating the response fields almost completely shifted when either eye or target was moved (Figure 7F). HE and TH responses were largely separable and dominated by eye position or target position (Figures 7E, 7G, and 7H; HE, −173°; TH, −16°).

The population analysis of Figure 7 established that in PMd, all three vectors T_E, T_H, and H_E are encoded across a population of cells. However, individual PMd neurons will only encode reach plans in a relative position code if they encode the T_E, T_H, and H_E vectors simultaneously. To identify the extent to which individual PMd neurons simultaneously encode these vectors during reach planning, we examined the intersections of tuning properties for cells with a tuned inseparable response to at least one pair of variables. We found 63 PMd cells encoded at least one of the three vectors. Of these 63 cells, 23 (37%) encoded both T_E and T_H. Therefore, individual PMd cells encode target position with respect to the hand as well as with respect to the eye. A substantial fraction of these cells (16/23 [70%]) also encoded H_E, indicating that in PMd all three vectors could be encoded inseparably in individual cells. In contrast, only 22 PMd cells (22/63 [35%]) encoded a single vector. This shows that, as illustrated in the example PMd neuron (Figures 3 and 4), many individual PMd cells simultaneously encode multiple vectors in a relative position code.

In contrast to PMd, of the 31 MIP cells that were tuned to at least one vector, 24 cells (77%) encoded T_E and a substantial proportion of these (11/24 [46%]) encoded only that single vector. This reinforces the distinction that PMd cells tend to simultaneously encode multiple vectors while MIP cells tend to only encode one vector, target position with respect to the eye.

Finally, we wanted to establish whether PMd had a stronger representation of T_E, T_H, or H_E. To do this, we compared the tuning strength of the response matrices using the length of the resultant of the gradient analysis. We found the strength of TE tuning was not significantly different than TH tuning (t test, $p > 0.05$), indicating T_E and T_H are represented with equal strength. We also found the strength of TE tuning was not significantly different than HE tuning and also that the strength of TH tuning was not significantly different than HE tuning. Therefore, PMd encodes all three vectors, T_E, T_H, and H_E, with equal strength.

Discussion

We found that during the delay period before a reach, PMd neurons encode the target, hand, and eye in a relative position code. Contrasting results from parietal area MIP confirmed previous work showing cells in this area use an eye-centered code. We propose eye position signals in PMd could play a role in coordinating the hand with the eye by encoding their relative position. Below, we discuss this result in the context of hand-eye coordination, consider limitations of our result related to the specific task employed, and examine methodological differences between our study and other work.

Relative Position Codes for Coordination

Overall, temporal issues in coordination have received more attention than spatial ones. Work on synchronized interlimb movements shows that relative phase, obtained by subtracting the phase angles of each limb, is the central concept for characterizing different behavioral coordination modes (Swinnen, 2002). For example, during movements of the arms or legs, in-phase (relative phase = 0°) movements are more stable and accurate than any other phase relationship. Our finding of an explicit neural representation of relative

hand-eye position is an exciting spatial complement to this work, as relative position codes could provide a general solution to the spatial problem of coordinating different body parts.

Experience with engineered systems shows a major problem for coordination is the accumulation of errors in position estimation (Olfati and Murray, 2002). Errors in estimating relative position are greatest when the positions of the individual body parts are represented in absolute coordinates. When absolute positions are subtracted to calculate relative position, the errors in position estimation can accumulate and do not cancel. Representing body parts directly in terms of relative position helps solve this problem as it reduces the number of position estimates and cancels errors that would otherwise accumulate (Gamini Dissanayake et al., 2001). Computationally, relative position codes are also more efficient than those based on absolute positions (Csorba and Durrant-Whyte, 1997; Newman, 1999). This is because using relative position separates the problem of coordinating two effectors from the larger problem of controlling the whole body. This is a powerful simplification. Whether neurons also represent the relative position of other body parts, such as the left and right hand, and how these encodings depend on coordination requirements will be an interesting area for future work.

Spatial transformations for hand-eye coordination are the subject of a growing body of work (Crawford et al., 2004). The prevailing view is to consider these as feed-forward spatial transformations converting visual information, which enters the brain in eye-centered coordinates, into hand-centered coordinates, and finally muscle commands for the arm and hand. Recent work shows parietal area 5 may play a role in these transformations. Many cells in area 5 encode targets in both hand and eye coordinates (Buneo et al., 2002). In other words, they represent T_E and T_H and thus bear similarities to the findings for PMd. In the Buneo et al. (2002) study, extensive response maps like those in Figure 2 were made for five initial hand positions and five target positions, but not for a range of eye positions. Thus, this design did not allow the determination of whether area 5 also represents the relative position of the hand and eye, H_E. It will be interesting to determine whether area 5 is similar to PMd and represents all three vectors in a relative position code. One potential difference between area 5 and PMd is that in PMd we find the encoding of the hand in eye coordinates, H_E, is as strongly represented as both the reach vector, T_H, and the target position in eye coordinates, T_E. This may not be the case for area 5.

Since we find PMd encodes T_E, T_H, and H_E with equal strength, a new function for this area is apparent: the relative position code in PMd may be involved in invertible transformations between hand-centered and eye-centered representations. Figure 8 shows a schematic of an invertible transformation. Feed-forward transformations convert visual input in eye-centered coordinates into hand-centered movement commands. They can do this directly using the position of the hand in eye coordinates. This transformation is invertible because a feedback transformation can also be performed that converts hand-centered into eye-centered coordinates. It does this using eye position in hand coordinates. In this way, relative position codes can perform invertible transformations between eye-and hand-centered representations.

Although relative computations in extrinsic representations like this are simple, whether the brain builds these extrinsic representations from its intrinsic sources is a matter for future experiments and theoretical investigation.

How does PMd construct its relative position code? Whereas cells in MIP code targets in eye coordinates, some are gain modulated by limb position (Buneo et al., 2002), and this gain effect also appears to be encoded in eye coordinates (C.A. Buneo et al., 1998, Soc. Neurosci., abstract). These gain modulated MIP neurons can perform the required

coordinate transformation to relative position coordinates in PMd by convergence and appropriate weighting of inputs to PMd. The source of this gain signal can be obtained directly from the vision of the hand or from a somatosensory-posture signal. In the latter case, this hand-in-body signal could be converted into hand-in-eye coordinates using a gain field related to gaze-in-body (head-in-body plus eye-in-head).

By similar reasoning, H_E can be produced by T_H response fields that are gain modulated by target-in-eye signals. It seems more likely, though, that these vectors can be formed by the same sources as the hand-in-eye gain effects mentioned above. In each case, cortical connections between PMd and other sensory-motor areas are consistent with a role in these invertible transformations (Matelli et al., 1998). Moreover, TMS studies over PMd have been shown to induce temporary disruptions of hand-eye coordination (Van Donkelaar et al., 2002).

Context-Dependent Reference Frames

Movements are made under different constraints and in different behavioral contexts. At present, it is not clear how much the neural encoding of movements is sensitive to these factors. Constraining the position of the hand and eye before and during reaching to certain locations on a screen, as required for the reference frame dissociation task, could elicit specific strategies for doing the task, and these strategies in turn could influence neural activity in PMd. For the case of constraining eye position, this issue has been studied for neurons in area MIP by examining them under free-viewing conditions (Cisek and Kalaska, 2002). The conclusion was that the eye-centered encoding is preserved, and it will be interesting to determine whether a more complex encoding like a relative position code is also preserved when a subject is freely viewing (see below).

Context also plays an important role as movements may be defensive, aggressive, and made outside of a behavioral task altogether. These movements not only differ in their parameters, the speed, endpoint, and trajectory, but also in the affective context in which they are made (Graziano and Cooke, 2006). Recent work examining the role of the expected reward following movements has shown this can exert a powerful influence on neural activity during the plan period before the movement (Musallam et al., 2004; Platt and Glimcher, 1999; Sugrue et al., 2004). This makes it very likely that other changes in context will modulate neural activity. Although it is less clear how the reference frame of an area itself will change in response to these manipulations, it is important to keep in mind that the class of movements presented here is restricted and overly general conclusions should not be drawn.

Methodological Issues with Previous Work

Other work has investigated eye position signals in PMd without reporting the encoding of relative position. Boussaoud et al. (1998) reported significant eye position effects when eye position was varied across three locations on a screen and reaches were made with the hand starting at a button near the body. It is possible these eye position effects reflect the encoding of relative hand-eye position but that it was difficult to observe in this experiment because, unlike our experiments, the hand and eye were not in a common workspace and so the relative positions of the hand and eye were similar across different trial conditions. In addition, they did not independently vary the positions of different effectors across a range of values and apply a combination of SVD and gradient analyses to the resulting matrices. Using this or a similar procedure is important given the potential complexity of the spatial transformations present in the association cortices. The gradient analysis is similar to the crosscorrelation method used to measure shifts but is more sensitive, as noise in the response

fields cancels instead of accumulates and the method averages across multiple positions instead of just two.

Cisek and Kalaska (2002) studied eye position signals during free gaze as a monkey controlled a cursor using a manipulandum from one initial position to different target positions. They reported strong gaze-centered discharge in MIP but modest gaze-related discharge in PMd and argued that eye position signals in PMd, but not MIP, were strongly influenced by controlled fixation. However, their analysis did not take into account eye, hand, and target position. Our results indicate that gaze-related activity in PMd neurons depends on hand, eye, and target position. This means it is inappropriate to average neuronal responses during fixation periods with, for example, the target above the eye and the eye to the left of the hand with periods with the target above the eye and the eye to the right of the hand as they could have very different firing rates. Since inappropriate averaging of neuronal responses will reduce the strength of an effect, the degree to which eye position responses in PMd are influenced by controlled fixation remains unclear.

Experimental Procedures

Experimental Preparation

Two male rhesus monkeys (*Macaca Mulatta*) participated in the experiments. Each animal was first implanted with a head cap and eye coil under general anesthesia. In a second surgery, recording chambers were implanted in frontal and posterior parietal cortex in the right hemisphere of each animal. Structural magnetic resonance imaging was used to identify the position of the arcuate sulcus and intraparietal sulcus and guide placement of the recording chambers to give access to cortex medial to each sulcus (Figure 1C). At a subset of recording sites in the frontal chamber of each monkey, microstimulation through the recording electrode evoked movements of the hand, arm, and occasionally leg with a threshold >40 μA (330 Hz 400 μs monopolar pulse width) consistent with published reports for PMd (Crammond and Kalaska, 1994). At no site was a saccade elicited with a threshold below 80 μA. Single-cell recordings from PPC conformed to previously published reports from MIP (functionally defined as a part of PRR [Calton et al., 2002; Snyder et al., 1997]). All surgical and animal care procedures were done in accordance with National Institute of Health guidelines and were approved by the California Institute of Technology Animal Care and Use Committee.

Neural recordings were made using multiple-electrodemicrodrives (3 or 5 channel, Thomas Recordings, Germany). During each session neural activity from each electrode was passed through a head stage (×20, Thomas Recordings, Germany), filtered (1 Hz–10 kHz; custom), amplified (×500–1000; TDT Electronics, Gainesville, Florida), digitized (20 kHz; National Instruments, Texas), and continuously recorded to disk for further analysis (custom C and Matlab code).

Behavioral Tasks

Reaches were made with the left arm on a touch-sensitive screen (ELO Touch Systems, California) while maintaining fixation to isolate reach-related activation from saccade-related activation. Behavior was controlled using custom Labview (National Instruments, Texas) code running on a real-time PXI platform. Eye position was monitored with a scleral search coil (CNC Engineering, Washington). Visual stimuli were presented on an LCD display (LG Electronics, Korea) placed behind the touch screen. Red circles instructed the animal where to fixate the eye. Green circles instructed the animal where to touch. All trials began with the illumination of a red and green circle which the animal needed to fixate with his eye and touch with his hand, respectively, and hold for a baseline period (~1000 ms). A

second green circle was then illuminated indicating the target of the reach. A delay period (~1000 ms) followed during which the animal had to withhold his response. After this the initial green circle the animal had to touch was extinguished providing the go signal for the animal to reach to the green target while maintaining fixation on the initial red circle. After the reach, the animal had to touch the second green circle while maintaining fixation on the red circle for 300 ms.

The spatial configurations of the initial eye position, initial hand position, and target position were independently varied across a range of values. Initial eye position was varied across four locations spaced 10° on a horizontal line, initial hand position was varied across the same four locations, and target position was varied across four locations spaced 10° on a horizontal line either above or below the initial hand and eye positions (Figure 1A). Targets were placed above or below to best activate the cell(s) being recorded.

Data Collection

Cells were first isolated and, if stable, recorded during the center-out task for both reaches and saccades. After these initial experiments, if there was a significant response to either task, recordings proceeded to the reference frame task. Occasionally, cells were acquired on additional electrodes and recorded despite the fact they had no task response, or cells were lost during a recording. All cells recorded for an average of at least three trials per condition the reference frame task were included in the database regardless of task response.

Data Analysis

Spike events were extracted and classified from the broadband activity using custom Matlab code (The Mathworks, Natick, Massachusetts) during the recording session and resorted offline. To account for nonstationarity in the recordings, spike classification was done on a 100 s moving window, and clusters were tracked across windows. Occasionally there were periods when clusters were not isolated. Trials during those periods were marked, and these data were not subject to further analysis. The delay period was defined as the 500 ms interval starting 500 ms after target onset.

Response matrices were characterized with a combination singular value decomposition (SVD) and orientation analyses (Buneo et al., 2002; Pena and Konishi, 2001). For the eye-hand-target analysis, the response to pairs of variables was determined by holding the third variable constant at the response field peak and analyzing the resulting two-dimensional matrix. The SVD analysis was used to see if each variable was separable or not. The extent of the concentration of the response energy in the first singular value determines how well the matrix can be described by the outer product of any two vectors of the appropriate lengths. If the responses of the cell to the two variables are separable, the response energy is highly concentrated on the first singular value, and the two vectors typically reflect the response of the neuron to each variable when considered separately. However, if the tuning of the cell for one variable shifts with the position of the other variable, the response energy will be less concentrated in the first singular value and the response is determined to be inseparable. Therefore, separability was defined by a significantly ($p < 0.05$) large first singular value compared to the first singular value calculated when trial conditions were randomized (randomization test). Thus, instead of referring to the strength of separability, which would be given by the magnitude of the first singular value compared with the others, we classified tuned responses as separable or inseparable according to the $p = 0.05$ threshold. A mean value was subtracted from the response matrix before performing the SVD. Gradient analysis was used to determine the orientation of the response field by computing the two-dimensional gradient of the response (estimated using the Matlab gradient function), doubling the angles to account for symmetric response fields, and

summing the gradient elements. The response to pairs of variables was considered tuned if the resultant gradient length was significantly greater than the length of the resultant gradient when trial conditions were randomized (randomization test). We used a two-way ANOVA to measure tuning and found it gave consistent results. Analyses utilizing all three dimensions of the data simultaneously were carried out by estimating the orientation of the spherical gradient. Unfortunately, symmetry considerations meant that, when estimating the orientation of the gradient, the vertical axis had to be treated differently than the horizontal axes. This meant that three gradients were still needed to characterize the data, so the more intuitive analyses based on two-dimensional gradients were used instead.

Idealized neuronal responses were created for eye-centered, hand-centered, and relative-position cells using the following formulae, where E gives eye position on the touch screen, H gives hand position on the touch screen, and T gives target position on the touch screen:

$$\text{eye-centered cell, } \frac{1}{1+\exp\left(\frac{H}{1000}\right)}\exp\left(\frac{-(T-E)^2}{500\pi}\right);$$

$$\text{hand-centered cell, } \frac{1}{1+\exp\left(\frac{E}{1000}\right)}\exp\left(\frac{-(T-H)^2}{500\pi}\right);$$

$$\text{relative-position cell, } \exp\left(\frac{-(T-E)^2}{500\pi}\right)\exp\left(\frac{-(T-H)^2}{500\pi}\right)\exp\left(\frac{-(H-E)^2}{500\pi}\right).$$

Acknowledgments

We would like to acknowledge valuable conversations with Chris Buneo and helpful comments on the manuscript from Alex Gail and Sam Musallam. This work was supported by NIH grants EY05522-21 and MH62528-01, the DARPA BioInfoMicro program, and a Career Award in the Biomedical Sciences from the Burroughs Wellcome Fund to B.P. We thank Tessa Yao for editorial assistance, Kelsie Pejsa and Leah Martel for animal care, and Viktor Shcherbatyuk for technical assistance.

References

Andersen RA, Buneo CA. Intentional maps in posterior parietal cortex. Annu. Rev. Neurosci. 2002; 25:189–220. [PubMed: 12052908]

Andersen RA, Essick GK, Siegel RM. Encoding of spatial location by posterior parietal neurons. Science. 1985; 230:456–458. [PubMed: 4048942]

Barash S, Bracewell RM, Fogassi L, Gnadt JW, Andersen RA. Saccade related activity in the lateral intraparietal area. II. Spatial properties. J. Neurophysiol. 1991b; 66:1109–1124. [PubMed: 1753277]

Batista AP, Buneo CA, Snyder LH, Andersen RA. Reach plans in eye-centered coordinates. Science. 1999; 285:257–260. [PubMed: 10398603]

Boussaoud D, Jouffrais C, Bremmer F. Eye position effects on the neuronal activity of dorsal premotor cortex in the macaque monkey. J. Neurophysiol. 1998; 80:1132–1150. [PubMed: 9744928]

Buneo CA, Andersen RA. The posterior parietal cortex: sensorimotor interface for the planning and online control of visually guided movements. Neuropsychologia. 2005:in press. Published online November 21, 2005. 10.1016/j.neuropsychologia.2005.10.011.

Buneo CA, Jarvis MR, Batista AP, Andersen RA. Direct visuomotor transformations for reaching. Nature. 2002; 416:632–636. [PubMed: 11948351]

Calton JL, Dickinson AR, Snyder LH. Non-spatial, motor-specific activation in posterior parietal cortex. Nat. Neurosci. 2002; 5:580–588. [PubMed: 12021766]

Caminiti R, Johnson PB, Burnod Y, Galli C, Ferraina S. Shift of preferred directions of premotor cortical cells with arm movements performed across the workspace. Exp. Brain Res. 1990; 83:228–232. [PubMed: 2073945]

Caminiti R, Johnson PB, Galli C, Ferraina S, Burnod Y. Making arm movements within different parts of space: the premotor and motor cortical representation of a coordinate system for reaching to visual targets. J. Neurosci. 1991; 11:1182–1197. [PubMed: 2027042]

Cisek P, Kalaska JF. Modest gaze-related discharge modulation in monkey dorsal premotor cortex during a reaching task performed with free fixation. J. Neurophysiol. 2002; 88:1064–1072. [PubMed: 12163555]

Crammond DJ, Kalaska JF. Modulation of preparatory neuronal activity in dorsal premotor cortex due to stimulus-response compatibility. J. Neurophysiol. 1994; 71:1281–1284. [PubMed: 8201421]

Crawford JD, Medendorp WP, Marotta JJ. Spatial transformations for eye-hand coordination. J. Neurophysiol. 2004; 92:10–19. [PubMed: 15212434]

Csorba, M.; Durrant-Whyte, HF. New approach to map building using relative position estimates. Paper presented at SPIE; Orlando, FL. 1997.

DeSouza JF, Dukelow SP, Gati JS, Menon RS, Andersen RA, Vilis T. Eye position signal modulates a human parietal pointing region during memory-guided movements. J. Neurosci. 2000; 20:5835–5840. [PubMed: 10908625]

Duhamel JR, Goldberg ME, Fitzgibbon EJ, Sirigu A, Grafman J. Saccadic dysmetria in a patient with a right fronto-parietal lesion. The importance of corollary discharge for accurate spatial behaviour. Brain. 1992; 115:1387–1402. [PubMed: 1422794]

Fogassi L, Gallese V, di Pellegrino G, Fadiga L, Gentilucci M, Luppino G, Matelli M, Pedotti A, Rizzolatti G. Space coding by premotor cortex. Exp. Brain Res. 1992; 89:686–690. [PubMed: 1644132]

Fu QG, Suarez JI, Ebner TJ. Neuronal specification of direction and distance during reaching movements in the superior precentral premotor area and primary motor cortex of monkeys. J. Neurophysiol. 1993; 70:2097–2116. [PubMed: 8294972]

Gamini Dissanayake MWM, Newman P, Clark S, Durrant-Whyte HF, Csorba M. A solution to the simultaneous localization and map building (SLAM) problem. IEEE Trans. Rob. Autom. 2001; 17:229–241.

Goldberg ME, Bruce CJ. Primate frontal eye fields. III. Maintenance of a spatially accurate saccade signal. J. Neurophysiol. 1990; 64:489–508. [PubMed: 2213128]

Graziano MS, Gross CG. Spatial maps for the control of movement. Curr. Opin. Neurobiol. 1998; 8:195–201. [PubMed: 9635202]

Graziano MS, Cooke DF. Parieto-frontal interactions, personal space, and defensive behavior. Neuropsychologia. 2006; 44:845–859. [PubMed: 16277998]

Graziano MS, Yap GS, Gross CG. Coding of visual space by premotor neurons. Science. 1994; 266:1054–1057. [PubMed: 7973661]

Johnson PB, Ferraina S, Bianchi L, Caminiti R. Cortical networks for visual reaching: physiological and anatomical organization of frontal and parietal lobe arm regions. Cereb. Cortex. 1996; 6:102–119. [PubMed: 8670643]

Kakei S, Hoffman DS, Strick PL. Direction of action is represented in the ventral premotor cortex. Nat. Neurosci. 2001; 4:1020–1025. [PubMed: 11547338]

Kalaska JF, Scott SH, Cisek P, Sergio LE. Cortical control of reaching movements. Curr. Opin. Neurobiol. 1997; 7:849–859. [PubMed: 9464979]

Khan AZ, Pisella L, Rossetti Y, Vighetto A, Crawford JD. Impairment of gaze-centered updating of reach targets in bilateral parietal-occipital damaged patients. Cereb. Cortex. 2005; 15:1547–1560. [PubMed: 15746004]

Matelli M, Govoni P, Galletti C, Kutz DF, Luppino G. Superior area 6 afferents from the superior parietal lobule in the macaque monkey. J. Comp. Neurol. 1998; 402:327–352. [PubMed: 9853903]

Mays LE, Sparks DL. Dissociation of visual and saccade-related responses in superior colliculus neurons. J. Neurophysiol. 1980; 43:207–232. [PubMed: 6766178]

Medendorp WP, Goltz HC, Vilis T, Crawford JD. Gaze-centered updating of visual space in human parietal cortex. J. Neurosci. 2003; 23:6209–6214. [PubMed: 12867504]

Merriam EP, Genovese CR, Colby CL. Spatial updating in human parietal cortex. Neuron. 2003; 39:361–373. [PubMed: 12873391]

Musallam S, Corneil BD, Greger B, Scherberger H, Andersen RA. Cognitive control signals for neural prosthetics. Science. 2004; 305:258–262. [PubMed: 15247483]

Newman, PM. PhD thesis. Sydney, Australia: University of Sydney; 1999. On the solution to the simultaneous localization and map building problem.

Olfati, R.; Murray, RM. Distributed cooperative control of multiple vehicle formations using structural potential functions. Paper presented at Proc. of the 15th IFAC World Congress; Barcelona, Spain. 2002.

Pena JL, Konishi M. Auditory spatial receptive fields created by multiplication. Science. 2001; 292:249–252. [PubMed: 11303092]

Platt ML, Glimcher PW. Neural correlates of decision variables in parietal cortex. Nature. 1999; 400:233–238. [PubMed: 10421364]

Sereno MI, Pitzalis S, Martinez A. Mapping of contra-lateral space in retinotopic coordinates by a parietal cortical area in humans. Science. 2001; 294:1350–1354. [PubMed: 11701930]

Shadmehr, R.; Wise, SP. The Computational Neurobiology of Reaching and Pointing. Cambridge, MA: MIT Press; 2005.

Shen L, Alexander GE. Preferential representation of instructed target location versus limb trajectory in dorsal premotor area. J. Neurophysiol. 1997; 77:1195–1212. [PubMed: 9084590]

Snyder LH, Batista AP, Andersen RA. Coding of intention in the posterior parietal cortex. Nature. 1997; 386:167–170. [PubMed: 9062187]

Soechting JF, Buneo CA, Herrmann U, Flanders M. Moving effortlessly in three dimensions: does Donders' law apply to arm movement? J. Neurosci. 1995; 15:6271–6280. [PubMed: 7666209]

Sugrue LP, Corrado GS, Newsome WT. Matching behavior and the representation of value in the parietal cortex. Science. 2004; 304:1782–1787. [PubMed: 15205529]

Swinnen SP. Intermanual coordination: from behavioral principles to neural-network interactions. Nat. Rev. Neurosci. 2002; 3:350–361.

Tweed D, Vilis T. Implications of rotational kinematics for the oculomotor system in three dimensions. J. Neurophysiol. 1987; 58:832–849. [PubMed: 3681398]

Van Donkelaar P, Lee J-H, Drew AS. Eye-hand interactions differ in the human premotor and parietal cortices. Hum. Mov. Sci. 2002; 21:377–386. [PubMed: 12381394]

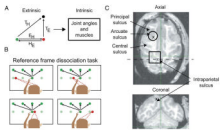

Figure 1. The Behavioral Task and Recording Sites

(A) Geometry of hand-eye coordination. Sensory-motor transformations generate movement plans in an extrinsic space, and nonlinear transformations convert these to an intrinsic space to generate accurate muscle commands.

(B) The reference frame dissociation task. A reach without a saccade is made from one of four hand positions on a line to one of four target positions while fixation is maintained at one of four eye positions.

(C) Structural magnetic resonance images from one monkey showing recording chamber placement with respect to sulcul landmarks. “X” marks the mean recording location in each chamber.

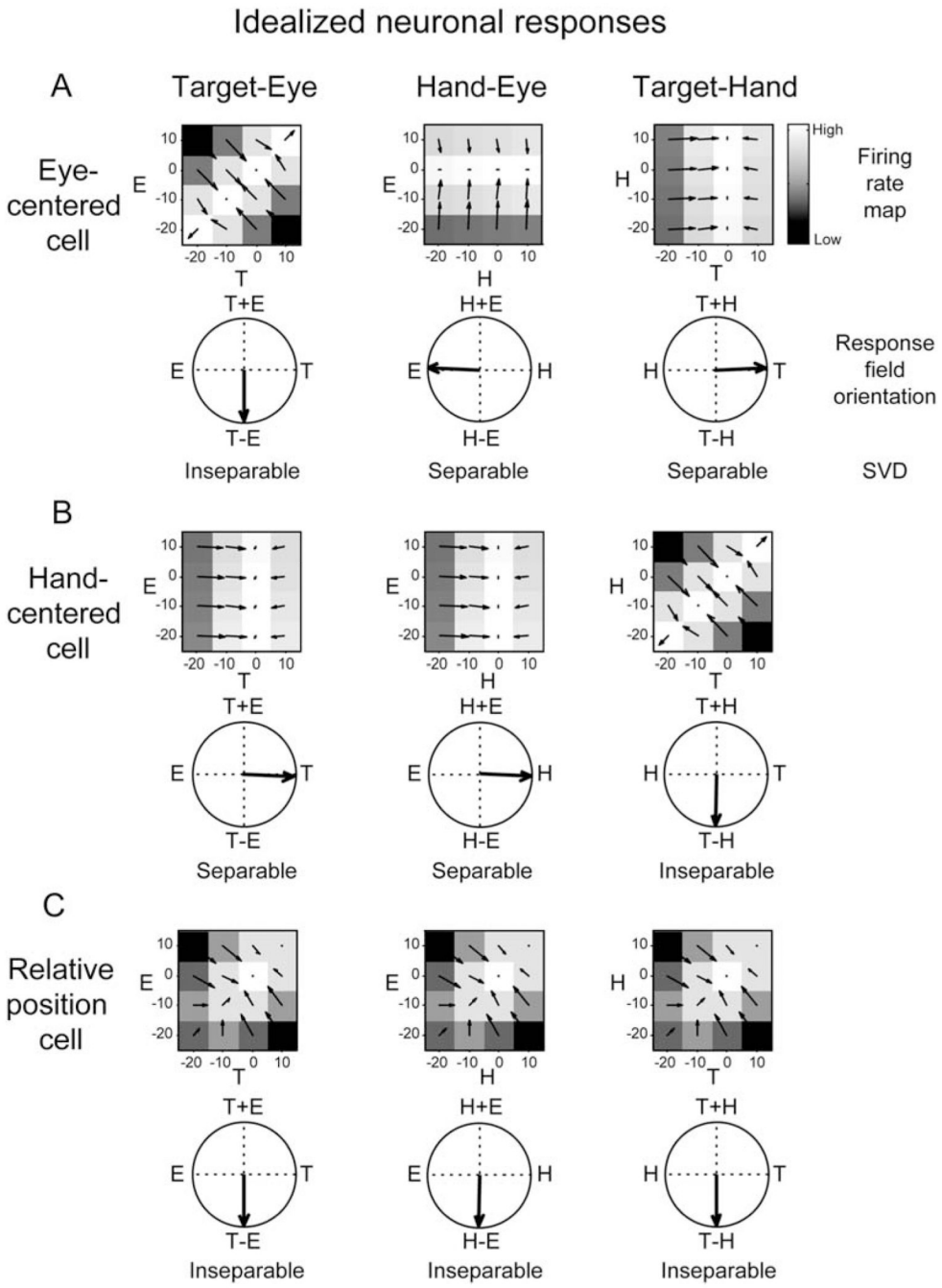

Figure 2. Idealized Cell Responses with Eye-Hand-Target Tuning for Cells with Three Different Reference Frames

(A) An eye-centered cell whose response is modeled as a gain field of hand position modulating eye-centered tuning.

(B) A hand-centered cell whose response is modeled as a gain field of eye position modulating hand-centered tuning.

(C) A relative-position cell whose response is modeled as a product of eye-centered, hand-centered, and relative eye-hand position tuning.

Arrows on each response field matrix are the gradient of the firing rate so that components of each arrow show how much the firing rate changed when each variable changed. The

separability, from the SVD, and the response field orientation, from the gradient analysis, (see Experimental Procedures) are shown for each idealized cell. The SVD yields an inseparable result when the outer product multiplication of any two vectors cannot describe the response matrix well. The gradient analysis quantifies how much the response to one variable shifts as the other changes position. 0° points right, and angles increase counterclockwise. White = high firing rate. Black = low firing rate. These conventions are also used below (Figures 4 and 6).

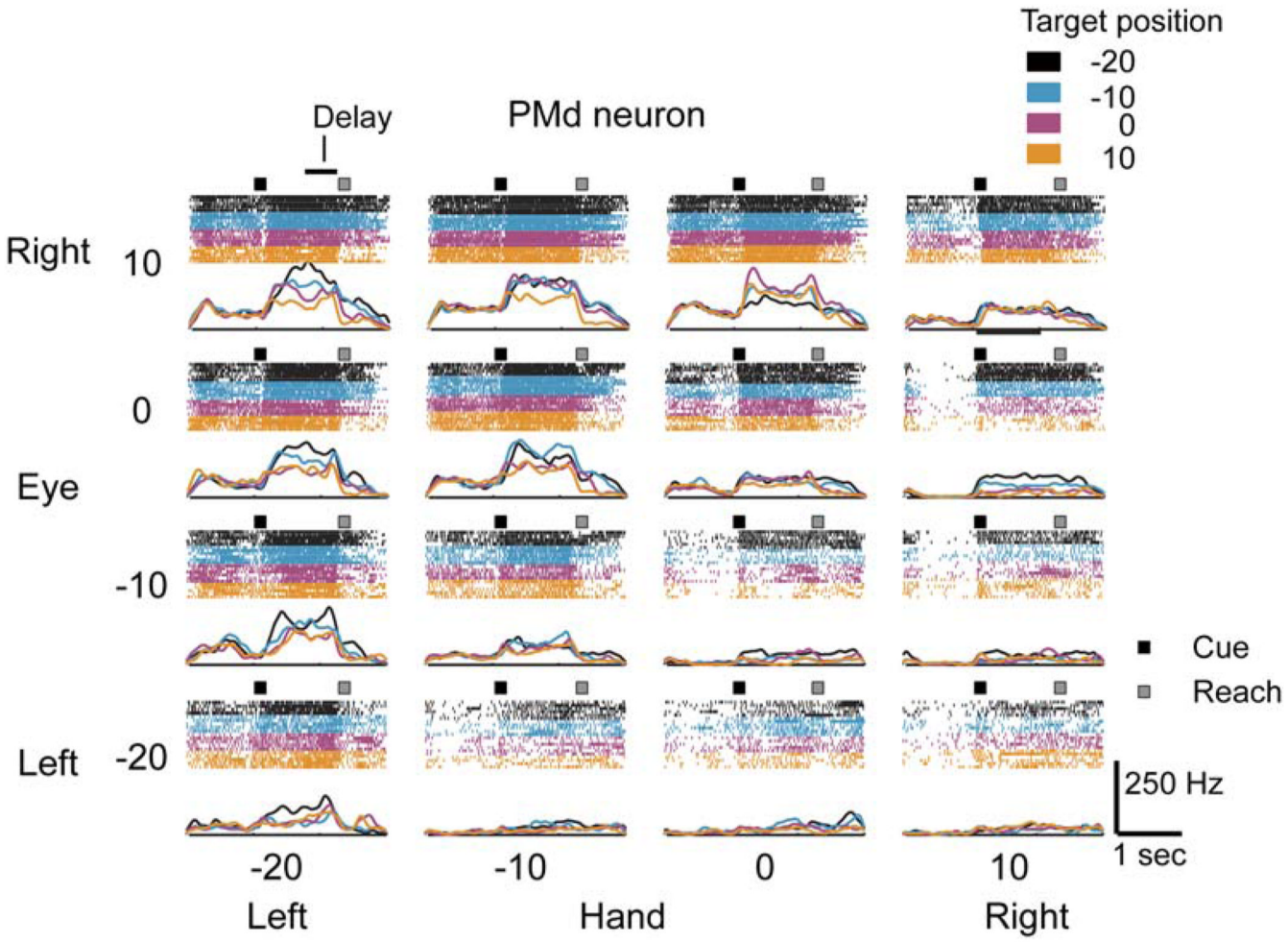

Figure 3. Example PMd Cell

Responses to the reference frame dissociation task are aligned to target onset (black square) as eye position is varied (rows), hand position is varied (columns), and target position is varied (within each panel). Eye (E), hand (H), and target (T) positions are shown above each panel. Spike rasters are shown above the panel color-coded for each target position in that panel. Target onset time (black square) and mean movement onset time (gray square) are shown on each panel. The horizontal bar on the top left panel indicates the delay period analysis interval.

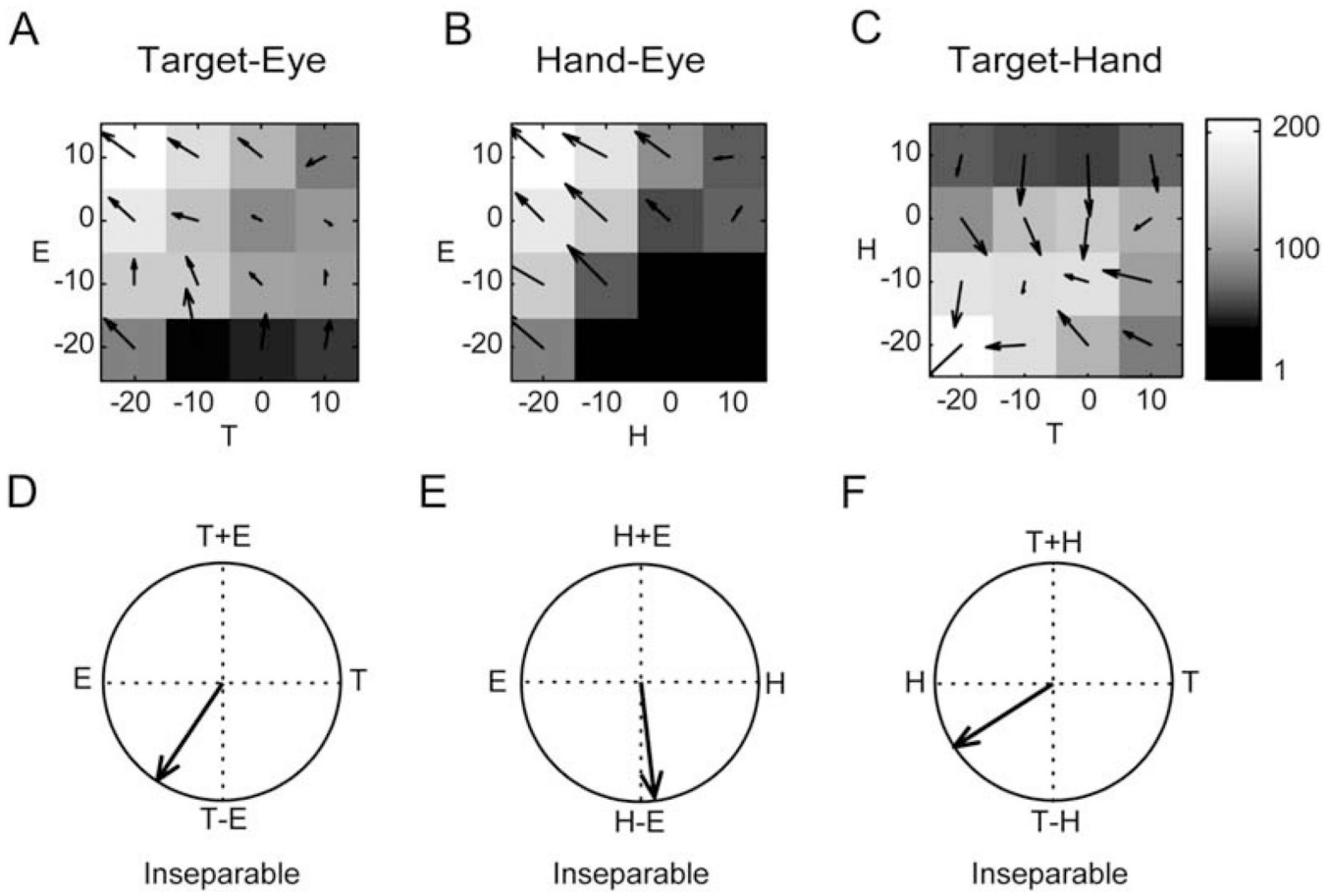

Figure 4. Example PMd Cell Eye-Hand-Target Response Matrices

(A) Target-eye response matrix during the delay period at the peak of the response field. The hand is at 20°. Arrows show the two-dimensional gradient elements.

(B and C) Similar for target-hand and hand-eye response matrices with the eye at 10° and the target at −20°, respectively.

(D) Overall response field orientation for the TE response matrix, −130°.

(E) Overall response field orientation for the TH response matrix, −146°.

(F) Overall response field orientation for the HE response matrix, −77°. 0° points right and angles increase counterclockwise.

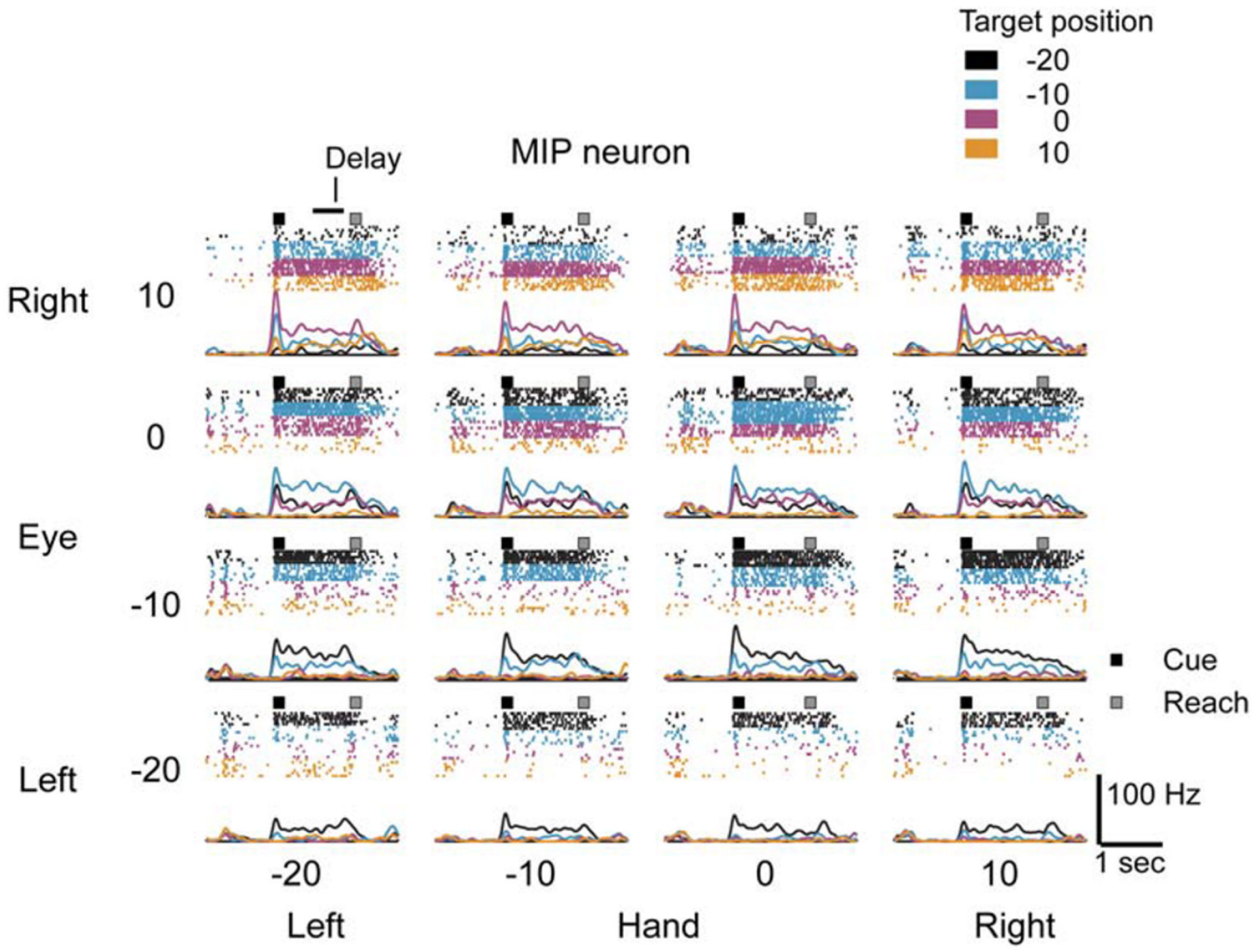

Figure 5. Example MIP Cell

Responses to the reference frame dissociation task are aligned to target onset (black square) as eye position is varied (rows), hand position is varied (columns), and target position is varied (within each panel). Eye (E), hand (H), and target (T) positions are shown above each panel. Spike rasters are shown above the panel color-coded for each target position in that panel. Target onset time (black square) and mean movement onset time (gray square) are shown on each panel. The horizontal bar on the top left panel indicates the delay period analysis interval.

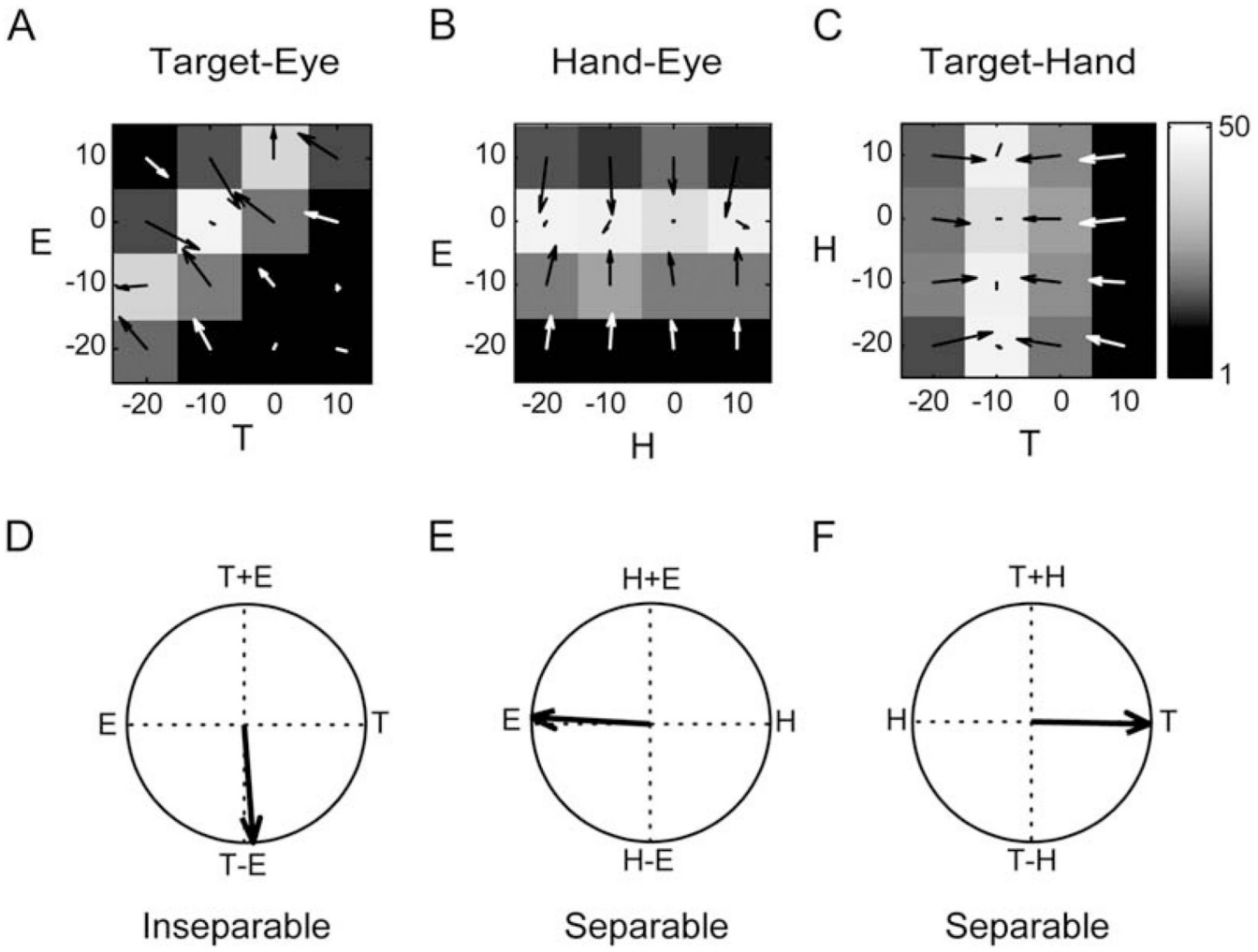

Figure 6. Example MIP Cell Eye-Hand-Target Response Matrices

(A) Target-eye response matrix during the delay period at the peak of the response field. The hand is at −20°. Arrows show the two-dimensional gradient elements.

(B and C) Similar for target-hand and hand-eye response matrices with the eye at 0° and the target at −10°, respectively.

(D) Overall response field orientation for the TE response matrix, −86°.

(E) Overall response field orientation for the TH response matrix, 0°.

(F) Overall response field orientation for the HE response matrix, 177°. 0° points right and angles increase counterclockwise.

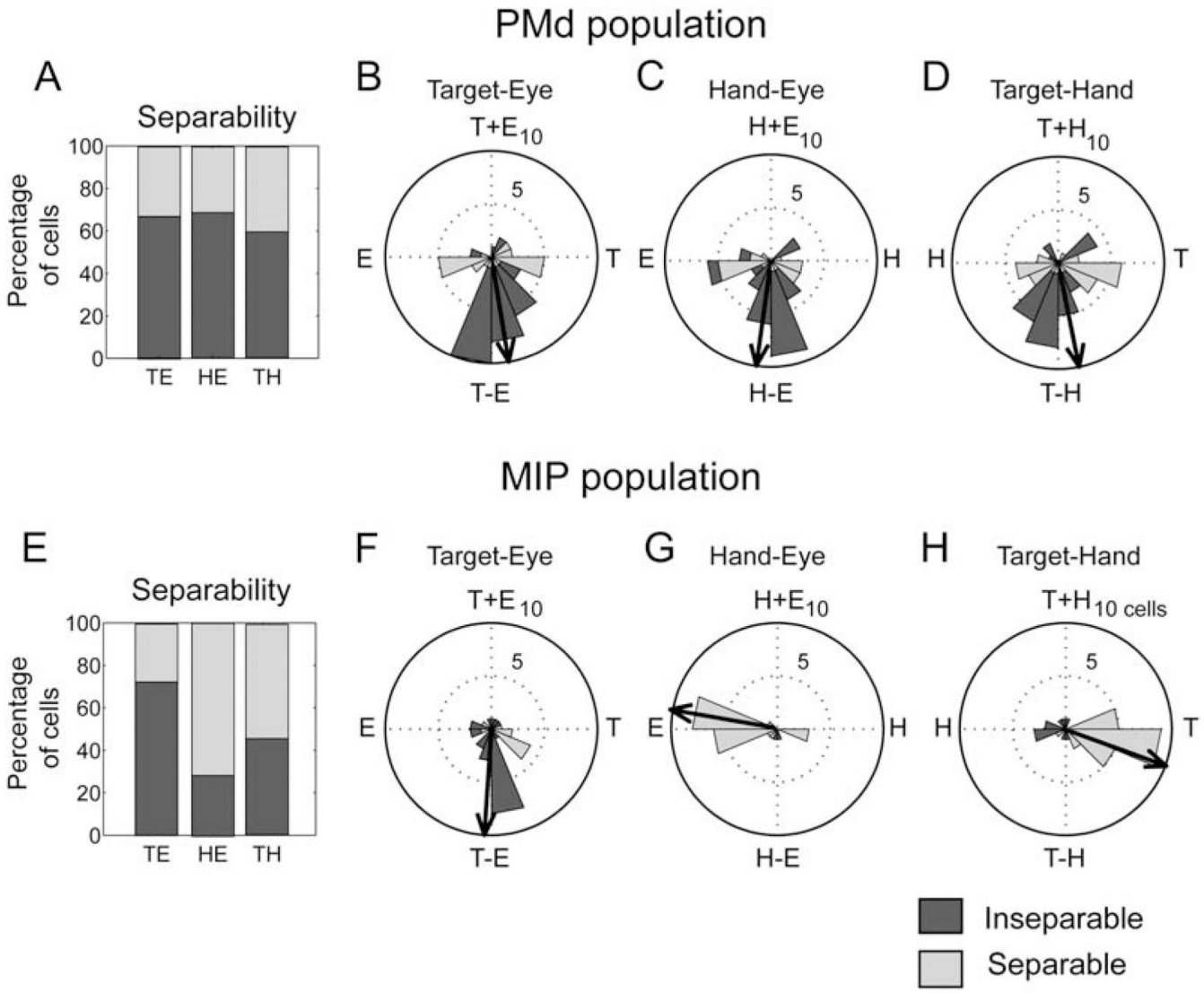

Figure 7. Population Eye-Hand-Target Analysis during the Delay Period

(A) Population separability for all PMd cells with tuned delay-period responses. The percentage of inseparable cells is shown in dark gray. The percentage of separable cells is shown in light gray. Population histograms for (B) eye-target response field orientation, (C) eye-hand response field orientation, and (D) hand-target response field orientation for tuned PMd neurons. Orientations for inseparable cells are shown in dark gray. Orientations for separable cells are shown in light gray.

(E–H) Same for tuned MIP neurons.

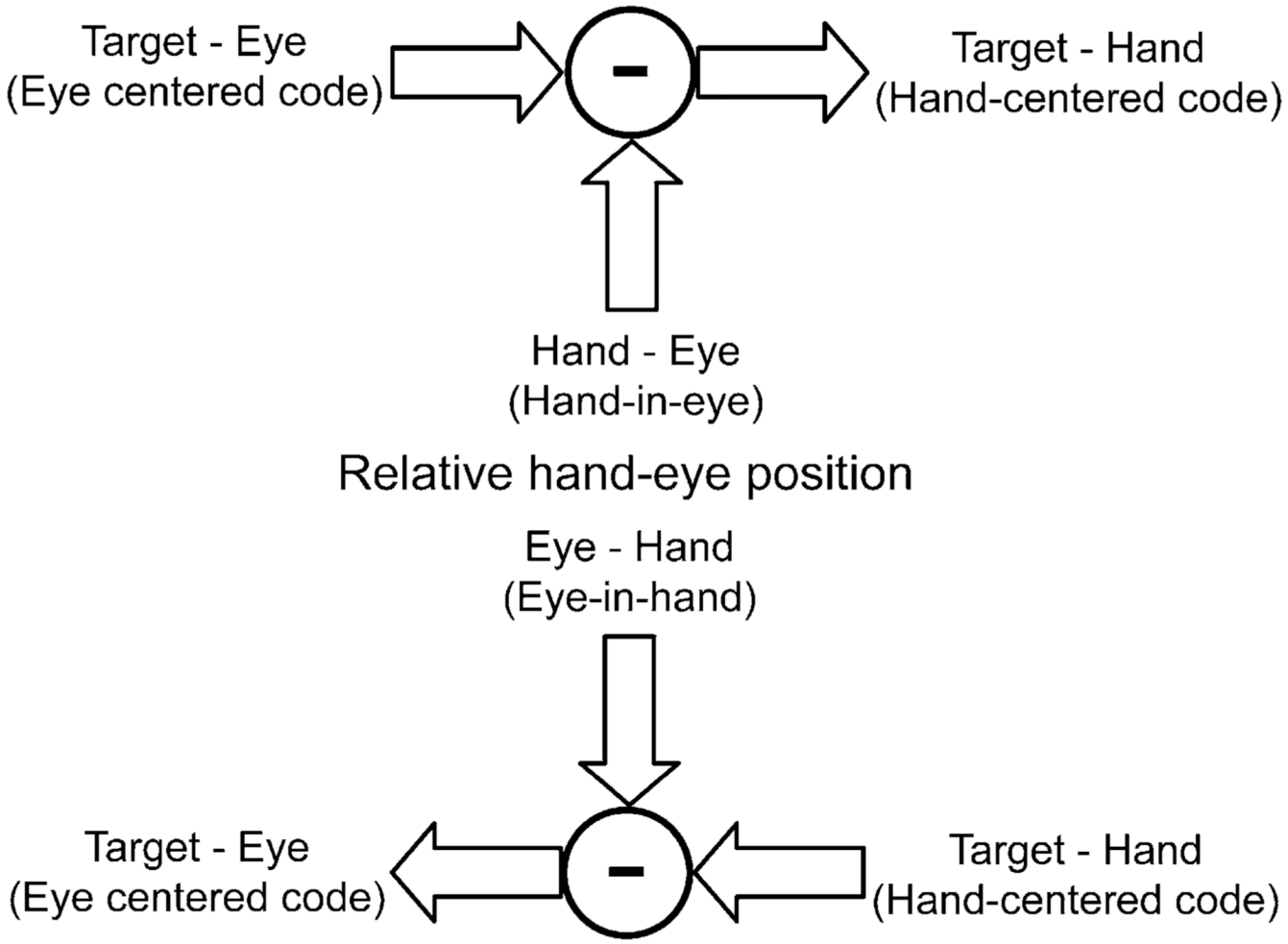

Figure 8. Schematic for Invertible Transformations

Schematic showing how a relative position code performs invertible sensory-motor transformations between eye-centered and hand-centered reference frames.